Contents

1
Methods

1.1 Abstract

We describe the technical details of the algorithms used to compute quantities of interest. We report the convergence behaviour of the algorithms and discuss validity and sources of error.

1.2 Technical details

For the models treated in this thesis, the corner transfer matrix A and the row-to-row transfer matrix T are symmetric. But due to the accumulation of machine-precision sized errors in the matrix multiplication and singular value decomposition, this will, after many algorithm steps, no longer be the case. In order for results to remain valid, we manually enforce symmetricity after each step.

The tensor network contractions at each algorithm step will cause the elements of A and T to tend to infinity, which means that they will at some point exceed the maximum value of a floating point number as it can be stored in memory. But because the elements of A and T represent Boltzmann weights, they can be scaled by a constant factor, which allows us to prevent this overflow if we use a suitable scaling. For example by requiring that

$$\mathrm{Tr}\, A^4 = 1, \tag{1.1}$$

so that the interpretation of A^4 as a reduced density matrix of an effective one-dimensional quantum is valid.

1.3 Convergence criteria

1.3.1 Simulations with finite bond dimension

The convergence of the CTMRG algorithm with fixed bond dimension m (the infinite system algorithm) can be defined in multiple ways (*cite*). In this thesis, the convergence after step i of the algorithm is defined as

$$c_i = \sum_{\alpha=1}^{m} |s_\alpha^{(i)} - s_\alpha^{(i-1)}|, \tag{1.2}$$

where s_α are the singular values of the corner transfer matrix A. If the convergence falls below some threshold ϵ, the algorithm terminates.

The assumption is that once the singular values stop changing to some precision, the optimal projection is sufficiently close to its fixed point and the transfer matrices A and T represent an environment only limited by the length scale given by m, i.e.

$$\xi(m) \ll N \tag{1.3}$$

is satisfied.

Convergence at the critical point of the Ising model

The convergence is shown in Figure 1.1. It is clear that the phenomenological law

$$\log c_n \propto n \tag{1.4}$$

holds to high precision, with the slope depending on m. Deviations only occur at values of c of around 10^{-12}.

The convergence of the various quantities as function of the number of algorithm steps is shown in Figure 1.2. For all quantities Q, the absolute relative difference with the final algorithm step

$$\Delta Q_{\mathrm{rel}}(n) = \left| \frac{Q(n) - Q(n = 10^5)}{Q(n = 10^5)} \right| \tag{1.5}$$

is shown. Again, a law of the form

$$\log(\Delta Q_{\mathrm{rel}}) \propto n \tag{1.6}$$

seems to hold.

To make an estimate of a quantity in the limit $N \to \infty$, or equivalently $\epsilon \to 0$, we can study the change in a quantity as function of the convergence threshold ϵ. We define

$$\Delta Q(\epsilon) = M(\epsilon) - M(10\epsilon), \tag{1.7}$$

i.e. the change of quantity Q when we decrease the threshold ϵ by an order of magnitude. The results in Figure 1.3 show that, remarkably, the order parameter, entropy and correlation length to high precision follow the linear relationship

$$\Delta Q(\epsilon) = \alpha_1(m)\epsilon, \tag{1.8}$$

whereas the free energy follows a quadratic relationship

$$\Delta f(\epsilon) = \alpha_2(m)\epsilon^2. \tag{1.9}$$

This means that we can confidently extrapolate the value of a quantity in the fully converged limit as

$$Q(\epsilon \to 0) = Q(\epsilon_{\min}) + \sum_{\epsilon = \frac{\epsilon_{\min}}{10}, \frac{\epsilon_{\min}}{100}, \ldots} \Delta Q(\epsilon), \tag{1.10}$$

where $\epsilon_{\min}$ is the lowest threshold used in simulation, and $\Delta Q(\epsilon)$ is determined by fitting to suitable higher values of the threshold.

technically this is not correct for the already converged values of m

Cross check with correlation length, report on boundary conditions

1.3.2 Simulations with finite system size

In the finite-system algorithm, we want to reliably extrapolate quantities in the bond dimension m. The convergence behaviour is shown in Figure 1.4. For each quantity Q, we plot the absolute relative difference with the value at the highest m

$$\Delta Q_{\text{rel}}(m) = \left| \frac{Q(m) - Q(m = 200)}{Q(m = 200)} \right| \tag{1.11}$$

versus the bond dimension m.

The plateaus of m-values that barely increase the precision are due to the degeneracies in the spectrum of the reduced density matrix. Apart from this structure, the law

$$\Delta Q_{\text{rel}}(m) \propto m^{\alpha(N)} \tag{1.12}$$

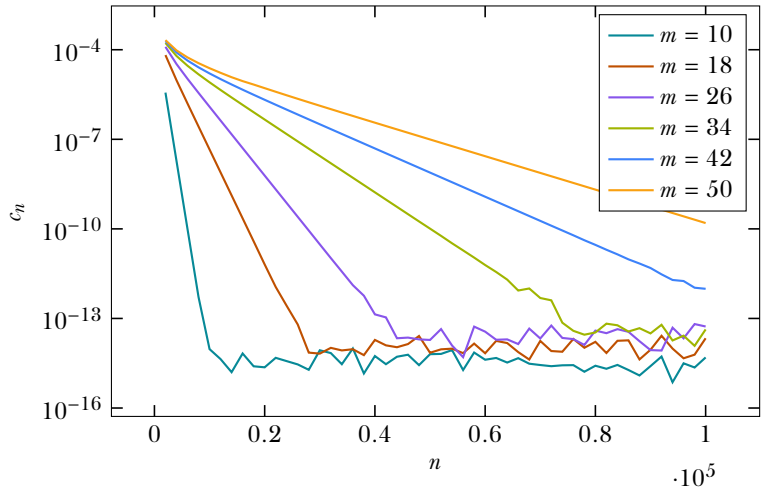

Figure 1.1: Convergence as defined in Equation 1.2 versus n, the number of CTMRG steps. Up until very small values of c_n, the convergence is monotonically decreasing and obeys a logarithmic law with slope depending on m.

is seen to hold for high enough m for the order parameter, free energy and entropy.

To extrapolate to $m \to \infty$, analogously to the finite-m case we define

$$\Delta Q_{\text{step}}(m) = Q(m) - Q(m-1) \tag{1.13}$$

Why does the free energy converge much faster?

1.4 Spectrum of the corner transfer matrix

1.4.1 Analytical results for the Ising model

In what follows, we present results established in [1, 2].

For the off-critical Ising model on a square lattice, we have [3]

$$\hat{\rho} = \hat{A}^4 = \exp(-\hat{H}_{\text{CTM}}), \tag{1.14}$$

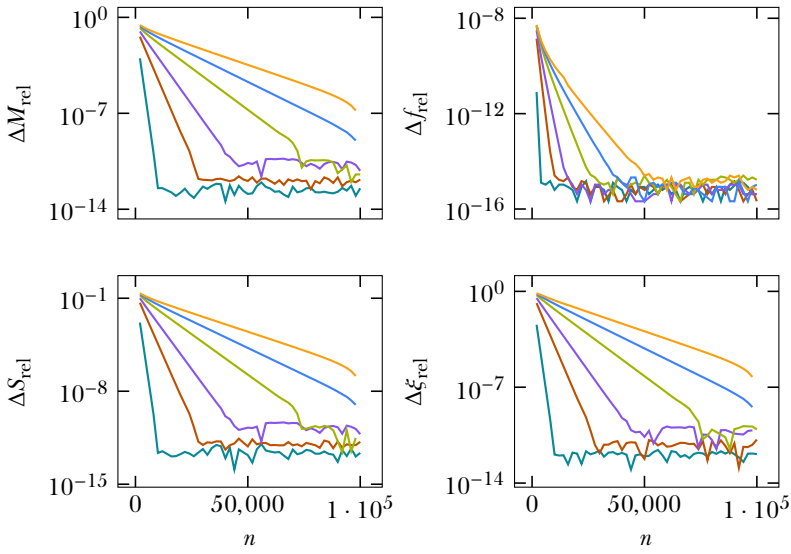

Figure 1.2: Absolute relative difference of quantities (see Equation 1.5). Same legend as Figure 1.1.

where

$$\hat{H}_{\text{CTM}} = \sum_{l=0}^{\infty} \epsilon_l(T) c_l^{\dagger} c_l, \tag{1.15}$$

with c_l and $c_l^{\dagger}$ fermionic annihilation and creation operators and

$$\epsilon_l = \begin{cases} (2l+1)\epsilon(T) & \text{if } T > T_c, \\ 2l\epsilon(T) & \text{if } T < T_c. \end{cases} \tag{1.16}$$

with $\epsilon(T)$ a model-specific factor that only depends on temperature.

In other words, the reduced density matrix (or equivalently, the corner transfer matrix A) can be written as a density matrix of an effective free fermionic Hamiltonian with equally spaced excitations.

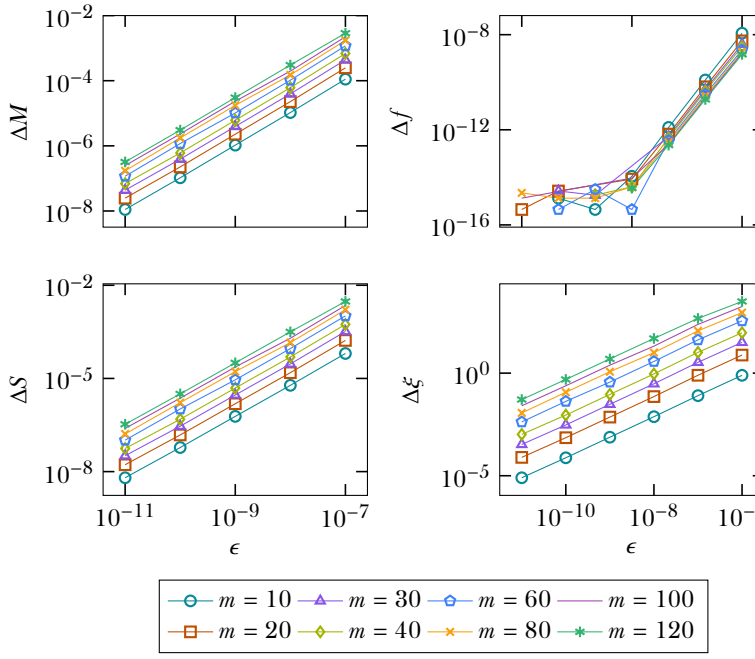

Figure 1.3: Stepwise differences upon decreasing the threshold ϵ by an order of magnitude, as in Equation 1.7. For the order parameter, entropy and correlation length, a linear relationship holds to high precision, while for the free energy the relationship is quadratic.

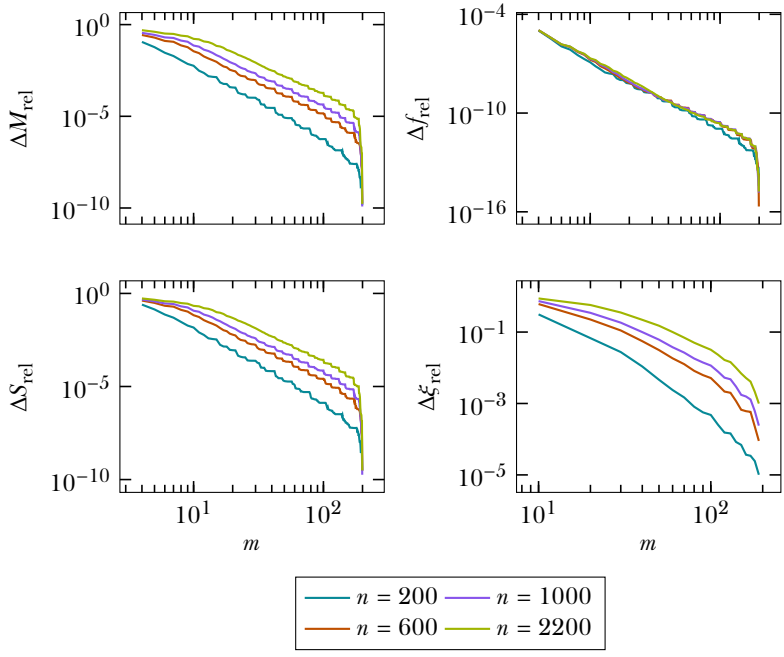

Figure 1.4: The absolute relative difference of quantities, as defined in Equation 1.11. For high enough m, it obeys a power law with varying exponent $\alpha(N)$. The sharp drop for the highest values of m is an artefact of the definition of ΔQ_{rel} and the plateau-like fashion in which the value of a quantity converges, owing to the spectrum of the reduced density matrix approximated by the CTMRG algorithm. Like in the finite-m case, the free energy converges much faster than the other quantities, and does so with little n-dependence. Note that $\Delta\xi_{\mathrm{rel}}$ does not obey a power law.

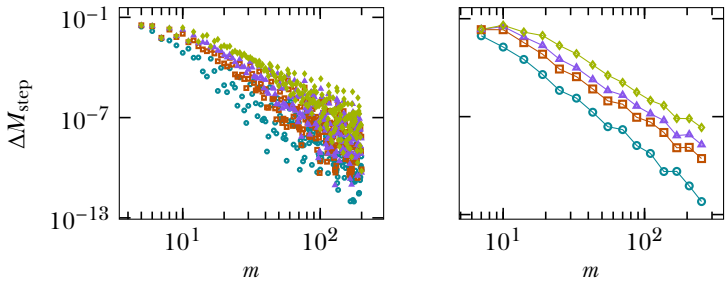

Figure 1.5: hallo

What does this mean for the spectrum of A? If we assume a free boundary, we have to distinguish between the ordered and disordered phase.

In the disordered phase, we have $\epsilon_l = (2l + 1)\epsilon(T)$. The ground state, $E = 0$, corresponds to the vacuum state of the effective system described by H_{CTM}. The single-fermion excitations give ϵ, 3ϵ, 5ϵ, ..., while two-fermion excitations give 4ϵ ($c_0^\dagger c_1^\dagger |0\rangle$), 6ϵ ($c_0^\dagger c_2^\dagger |0\rangle$) and 8ϵ ($c_0^\dagger c_3^\dagger |0\rangle$ *or* $c_1^\dagger c_2^\dagger |0\rangle$). So the first degeneracy appears at 8ϵ. 9ϵ is also degenerate: it can be constructed with a single-fermion excitation ($c_4^\dagger |0\rangle$) and a three-fermion excitation ($c_2^\dagger c_1^\dagger c_0^\dagger |0\rangle$).

The numerical results from the CTMRG algorithm exactly confirm this picture. See the $T = 2.6$ line in the left panel of Figure 1.6. The gap after the first two eigenvalues is due to the absence of the level 2ϵ. The ϵ_l are linear and the degeneracies are correct.

In the ordered phase, we have a two-fold degeneracy for every state due to symmetry and ground state energy $E = 0$. After that, the only available levels are 2ϵ, 4ϵ, 6ϵ, ... The degeneracy of the nth energy level is given by $2p(n)$, twice the number of partitions of n into distinct integers [4], with the factor of two coming from symmetry.

To illustrate: $c_1^\dagger c_2^\dagger |0\rangle$ and $c_3^\dagger |0\rangle$ both have $E = 6\epsilon$, the third energy level (counting the vacuum as the zeroth energy level), which is to say $p(3) = 2$ since $\{3, 2 + 1\}$ are the ways to write 3. The line $T = 2$ in the left panel of Figure 1.6 confirms these results.

With a fixed boundary, the spectrum in the disordered phase doesn't change. In the ordered phase however, the two-fold degeneracy due to symmetry is

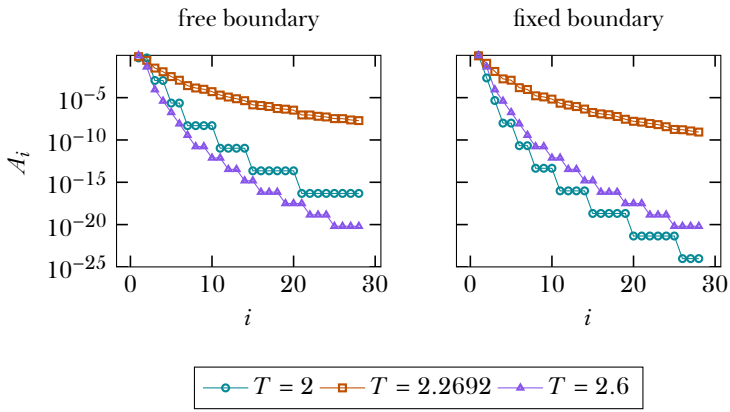

Figure 1.6: First part of the spectrum of A after $n = 1000$ steps with a bond dimension of $m = 250$.

lifted, so the degeneracy of the nth energy level becomes $p(n)$. As a consequence, the spectrum decays much faster. See the right panel of Figure 1.6.

At or close to criticality, the expression in Equation 1.14 breaks down, and the spectrum of $\hat{\rho}$ is smoothened out. In general, below and at criticality, the spectrum decays slower for a free boundary. This is to be expected, since A preserves the symmetry when the boundary is free. At $T = 0$, A has two equally large non-zero eigenvalues, representing either all up or all down spins on the boundary of the quadrant, while for a fixed boundary, A has one non-zero eigenvalue: it represents a completely polarized state.

Bibliography

[1] Ingo Peschel and Viktor Eisler. "Reduced density matrices and entanglement entropy in free lattice models". In: *Journal of physics a: mathematical and theoretical* 42.50 (2009), p. 504003.

[2] Ingo Peschel, Matthias Kaulke, and Örs Legeza. "Density-matrix spectra for integrable models". In: *Annalen der Physik* 8.2 (1999), pp. 153–164. ISSN: 1521-3889. DOI: 10.1002/(SICI)1521-3889(199902)8:2<153::AID-ANDP153>3.0.CO;2-N. URL: http://dx.doi.org/10.1002/(SICI)1521-3889(199902)8:2%3C153::AID-ANDP153%3E3.0.CO;2-N.

[3] Brian Davies. "Corner transfer matrices for the Ising model". In: *Physica A: Statistical Mechanics and its Applications* 154.1 (1988), pp. 1–20.

[4] Kouichi Okunishi, Yasuhiro Hieida, and Yasuhiro Akutsu. "Universal asymptotic eigenvalue distribution of density matrices and corner transfer matrices in the thermodynamic limit". In: *Physical Review E* 59.6 (1999), R6227.